Volume 9, Issue 6, 2019, 4655 - 4662 ISSN 2069-5837

Biointerface Research in Applied Chemistry

www.BiointerfaceResearch.com

https://doi.org/10.33263/BRIAC96.655662

Original Research Article Open Access Journal

Received: 29.10.2019 / Revised: 18.11.2019 / Accepted: 19.11.2019 / Published on-line: 21.11.2019

Fabrication of label-free electrochemical food biosensor for the sensitive detection of ovalbumin on nanocomposite-modified graphene electrode

Azureen Mohamad[1], Mohammad Rizwan[1,2], Natasha Ann Keasberry[1], Minhaz Uddin Ahmed[1,*]

[1]Biosensors and Biotechnology Laboratory, Chemical Science Programme, Faculty of Science, Universiti Brunei Darussalam, Brunei, Darussalam
[2]School of Natural Sciences, Bangor University, Bangor, Gwynedd, United Kingdom
[*]corresponding author e-mail address: ***minhaz.ahmed@ubd.edu.bn*** | Scopus ID 7402830936

ABSTRACT

In this work a highly sensitive label-free electrochemical food biosensor for the detection of egg allergen ovalbumin (Ova) was developed using nanocomposite consisting of iron oxide (Fe_3O_4) and palladium (Pd) nanoparticles with conducting polymer chitosan (CS). Pd nanoparticles were synthesized and seeded onto Fe_3O_4 nanoparticles, and dispersed in CS to form the nanocomposite. The nanocomposite (Fe_3O_4-Pd/CS) was drop-casted onto a screen printed graphene electrode (SPGE). Subsequently, 4-ABA was electrografted onto the modified SPGE/Fe_3O_4-Pd/CS. Carbodiimide chemistry was performed for the covalent conjugation of Ova-antibody (Ova-Ab) onto the electrode surface. The bimetallic nanocomposite portrayed excellent electrocatalytic effect due to the synergistic conductive effect of the Fe_3O_4-Pd nanomaterials and CS polymers and facilitated the electron movement between electrode surface and redox buffer. Additionally, ABA also enhanced electronic current on the surface of the electrode. Featuring high electron conductivity, the developed food biosensor demonstrated a large linear range to detect the Ova between 0.01 pg/mL – 1 µg/mL with a low limit of detection of 0.01 pg/mL. Furthermore, the proposed food biosensor portrayed very good selectivity with a high potential to detect Ova in real food sample.

Keywords: *Electrochemical; Food biosensor; Ovalbumin; Iron oxide nanoparticles; Palladium nanoparticles; Food allergies; screen printed graphene electrode; Nano-bio interface; Nanotechnology and applied nanoscience; Analytical chemistry; Electrochemistry.*

1. INTRODUCTION

The increase in prevalence of food allergies across the globe due to presence of chemical or microbial contaminants, or any undesirable substances has put the life of the consumers on risk [1]. The presence of chemical or microbial contaminants, or any undesirable substances in food is also known as food allergens. These allergens in food could be found universally or may be natural in origin, such as ovalbumin. Ovalbumin is one of the most abundant protein in egg that induces allergic reactions in individuals [2, 3]. Egg allergen is listed as one of the main food allergens for food labeling in the US Food and Drug Administration. Food allergens may cause severe adverse effects on consumers health such as rashes, anaphylaxis and diarrhea. Diarrhea could even be fatal, if not treated on time. For this reason, the strict regulation of food labelling is very important to provide the necessary information regarding the food allergens.

Therefore, the most effective way to protect consumer health is to strictly avoid food that contains specific allergens. However, even though egg-containing food items are properly labelled, trace amounts of egg protein may be found contaminated in food that is not listed to contain egg ingredients, such as from handling, or utensils used during processing. So, it is anticipated that strict food risk assessment will be extremely important to protect the consumer health. Therefore, it is very crucial to determine the level of ovalbumin in food samples through highly sensitive method.

Currently, there are various methods to detect ovalbumin allergen, such as electrophoresis, western blotting, and the most common method, ELISA. However, these methods have limited sensitivity, are tedious, and expensive. Recently electrochemical detection method has attracted attention in the determination of ultrasensitive detection of biomarkers using biosensors, in particular label-free electrochemical biosensor [4, 5]. Therefore, for detection of egg protein in food samples ovalbumin can be used as the biomarker for the fabrication of label-free electrochemical biosensor. Further, Label-free electrochemical biosensor can be achieved with high sensitivity, low cost, simple to operate and interpret, rapid results, which could be miniaturized, without the complication of labelling [6]. Therefore, in this work, we aim to fabricate a highly sensitive label-free electrochemical food biosensor for the detection of a very common food allergens (ovalbumin) on the Fe_3O_4-Pd/CS nanocomposite modified screen-printed graphene electrode (SPGE).

In electrochemical reactions, the electrode surface is where both the reaction site and electron movement occur. Hence, modifying the electrode significantly affects the activation effect of the electrochemical reaction both by providing larger surface area and a highly conductive medium for the electron movement [7]. Therefore, recently, various metallic, and conducting polymers have been employed in developing electrochemical biosensors and immunosensors. Among them Palladium nanoparticles (Pd-NPs) and Fe_3O_4 nanoparticles (Fe_3O_4-NPs) have attracted considerable attention from the researchers due to their unique properties. Pd-NP is a well-known metallic nanomaterial with high conductivity and catalytic performance [8-11]. Furthermore, Yang et al., (2006) showed that PdNP exhibited the most sensitive response compared to Au, Ag, and Pt upon fabrication onto screen printed electrode (SPE) [12]. However, individual Pd-NP can be unstable during electrochemical process and aggregate easily [13]. Li *et al* showed that the presence of

Fe_3O_4-NPs helped the dispersion state of Pd-NPs [14]. Fe_3O_4-NPs have also been shown to have excellent electrocatalytic properties [15-18]. Zhuang *et al* (2015) found that Fe_3O_4-NPs enhanced electron transfer by Fe ions released from hematite and magnetite, which act as electron shuttles [19]. In addition, compared to the utilization of single/mono-nanomaterial, nanocomposites consisting of two or more conducting nanomaterials have been shown to greatly improve the conductivity of electrochemical biosensors [20], and consequently the sensitivity of the sensors itself. The nanocatalyst Fe/Pd composite has been shown to greatly improve the electrochemical rate of dechlorination of chloroacetic acids or chlorophenols [21, 22]. However, to the best of our knowledge, there are no studies utilizing the Fe_3O_4-Pd nanomaterials in fabrication of label-free electrochemical biosensor.

In biosensor applications, nanomaterials are usually dispersed in a supporting matrix to further enhance the electrocatalytic and conductivity behavior, as well as to stabilize the sensor [23, 24]. These matrix also act as binder to anchor the nanomaterials onto the electrode surface. Among different supporting matrix, recently chitosan (CS) has emerged a favourite polymer in biosensor fabrication due to its biocompatibility, film-forming ability, and property to act as conducting medium and stabilizer of the nanomaterials [25, 26]. CS is a linear polysaccharide containing randomly distributed β-(1→4)-linked D-glucosamine and N-acetyl-D-glucosamine units obtained from deacetylation of natural chitin [27]. CS contains large number of different functional groups such as acetamido group, amino group, and hydroxyl group, which can act as electron donors [28]. Additionally, 4-aminobenzoic acid (4-ABA) was also intercalated in this experiment due to its electrochemical profile and for the functionalization of the electrode with carboxylic group for carbodiimide chemistry for conjugation of the detecting antibody.

Using the novel properties of the nanomaterials and polymer fabricated label-free electrochemical food biosensors on the Fe_3O_4-Pd/CS nanocomposite modified SPGE demonstrated high sensitivity with a lower limit of detection of 0.01 pg/mL and wide linear range of 0.01 pg/mL-1 µg/mL for the detection of the most common food allergens (ovalbumin). Additionally, biosensor portrayed excellent selectivity, repeatability, stability and potential to detect ovalbumin in real food sample.

2. MATERIALS AND METHODS

2.1. Chemicals.

Monoclonal anti-chicken egg albumin antibody (Ovalbumin), albumin from chicken egg white, bovine serum albumin (BSA) (≥98%) were obtained from Sigma-Aldrich (USA). Other chemicals such as 1-Ethyl-3-(3-dimethylaminopropyl) carbodiimide (EDC), N-hydroxysuccinimide (NHS), Dimethyl sulfoxide (DMSO), potassium ferrocyanide ($K_4Fe(CN)_6$), potassium ferricyanide ($K_3Fe(CN)_6$), potassium hexachloropalladate (IV) (K_2PdCl_6), tween-20, sodium azide (NaN_3), 4-aminobenzoic acid ($C_7H_7NO_2$), and sodium nitrite ($NaNO_2$) were also purchased from Sigma-Aldrich (USA). 85% deacetylated chitosan was obtained from Alfa Aesar (M.A). Glacial acetic acid ($C_2H_4O_2$) and L-ascorbic acid ($C_6H_8O_6$) were obtained from BDH chemicals (USA). 15-20 nm iron oxide (Fe_3O_4) nanoparticles were purchased from US Research nanomaterials Inc. (USA). The buffers used in the experiment are as follows: (a) phosphate buffered saline (PBS) buffer (pH 7.4) for preparation of antibody, protein dilutions, washing, and dissolving, (b) 0.1% NaN_3 in PBS buffer (w/v), (c) 5 mM $[Fe(CN)_6]^{3-/4-}$ in PBS buffer for electrochemical analysis, (d) washing buffer PBS-tween 20, (e) blocking buffer, PBS buffer containing 0.1% BSA in 0.1% NaN_3 (w/v). Egg-free biscuit was purchased locally from a supermarket. All preparations used distilled water obtained from a Millipore water purification system (18MΩ, Milli-Q, Millipore).

2.2. Instrumentation.

The electrochemical experiment and analyses were carried out using an Autolab PGSTAT101 (Eco Chemie, The Netherlands) potentiostat/galvanostat linked to a desktop computer with NOVA software version 1.1.0. A pre-fabricated disposable SPGE consisting of a three-electrode system was obtained from Dropsens Inc. (Spain). In this experiment, the working electrode was pre-modified with graphene. Graphene was selected as the SPGE working electrode material as it has been shown that graphene is an excellent conducting material with high surface area to volume ratio for electrochemical sensing [29]. To study composition of nanocomposite, field-emission electron microscopy (FE-SEM) JEOL, JSM-7610F (Japan) was used. Before FE-SEM analysis, sample was carbon coated for 60 s.

2.3. Preparation of Fe_3O_4-Pd nanomaterials.

Nanomaterials were prepared according to literature with modifications [30]. In brief, 200 mg Fe_3O_4 was mixed in 25 mL distilled water. Following that, 30 µL of 50 mM ascorbic acid were added into the mixture and mix well. After that, 300 µL of 10 mM K_2PdCl_6 were added dropwise whilst stirring. The mixture was left to stir for 3 h for the complete synthesis of the nanomaterials. After that, the nanomaterials were magnetically separated for 30 min. The supernatant was removed and the nanomaterials were resuspended in distilled water and stored at 4˚C in a glass vial.

2.4. Fabrication of food biosensor.

The as-synthesized Fe_3O_4-Pd nanomaterial was dispersed and suspended in 0.1% CS in acetic acid (w/v) to make a Fe_3O_4-Pd/CS nanocomposite. 6 µL of the nanocomposite were drop casted onto the working electrode for functionalization of the electrode through physisorption for 90 min. After that, *in-situ* functionalization of the working electrode with diazonium salt was carried out as described by Lim and Ahmed, (2015) [6]. 10 mg/mL 4-aminobenzoic acid was added dropwise to 2 mM of sodium nitrite with constant stirring to produce a diazonium salt. Next the mixture was then dropped onto the modified electrode. Subsequently, One cycle of cyclic voltammetry ranging between 1 to -0.1 V at a scan rate of 200 mV/s was applied to induce electrodeposition of the diazonium salt on the working electrode and functionalized the surface with carboxyl group (-COOH). After that, the electrode was rinsed with water and dried at room temperature. Following that, 10 µL of EDC/NHS (100 mM each) in DMSO was dropped onto the electrode and allowed to react for 1 h at room temperature. The electrode was washed with water and PBS. After that, 10 µL of 5 µg/mL anti-ovalbumin (Ova-Ab)

was dropped onto the functionalized electrode at room temperature for antibody immobilization. After 2 h, the electrode was washed with PBS-tween 20 and dried. Finally, 50 µL of blocking buffer was incubated onto the electrode for 45 min. The electrode was washed with PBS-tween 20, dried, and stored at 4˚C until needed as illustrated in Scheme 1.

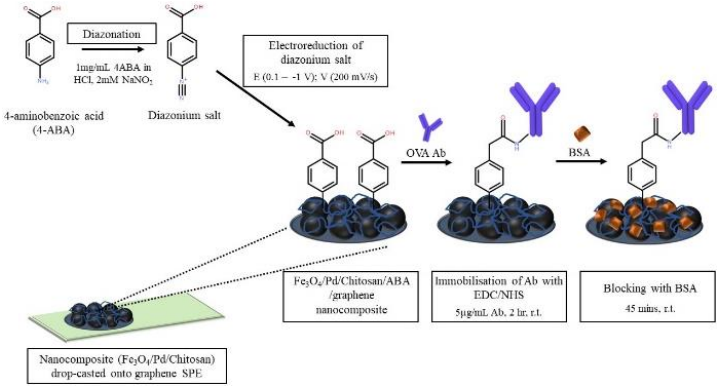

Scheme 2. Schematic illustration of food biosensor fabrication.

2.5. Electrochemical signal measurement.

10 µL of ovalbumin (Ova) at different concentrations were incubated onto the working electrode for 30 min at room temperature. The electrode was then washed with PBS-tween 20, and differential pulse voltammetry (DPV) readings were taken in $[Fe(CN)_6]^{3-/4-}$ between -0.1 to +0.4 V at 100 mV/s scan rate. The peak current at the different concentrations of Ova were calculated and used for analyses.

2.6. Preparation of sample for spike and recovery analysis.

Egg-free biscuit sample was crushed to form a homogenous mixture with mortar and pestle. 0.1 g of the biscuit sample was dispersed with 1 mL of PBS buffer and incubated at 60˚C. After 1 h, the sample was centrifuged at 3500 rpm for 10 min and the supernatant was collected. The supernatant was diluted 1:10000 in PBS buffer and spiked with different concentration of Ova (0.1, 10, 10000 pg/mL). Finally, the spiked extracts were incubated for 30 min with the food biosensor at room temperature and the DPV responses were recorded.

3. RESULTS

3.1. SEM characterization of nanomaterials and electrode surface.

SEM images of the Fe_3O_4 nanoparticles and Fe_3O_4-Pd nanomaterials are compared in Figure 1A and Figure 1B. The average diameter of the nanoparticles was observed to have increased in size suggesting that the Pd was successfully seeded onto the surface of Fe_3O_4 nanoparticles. In addition, the EDX spectrum showed the appearance of peaks due to Pd after the introduction of Pd onto Fe_3O_4 nanoparticles (supplementary materials, Figure S-1). The surface of the bare SPGE and Fe_3O_4-Pd/CS nanocomposite modified SPGE was also observed with SEM where the bare SPGE can be seen to have a flaky surface (Figure 1C), while in Figure 1D, the surface topology appeared smoother with speckles of well-dispersed nanocomposite, confirming that the SPGE was successfully coated with the Fe_3O_4-Pd suspended in CS matrix.

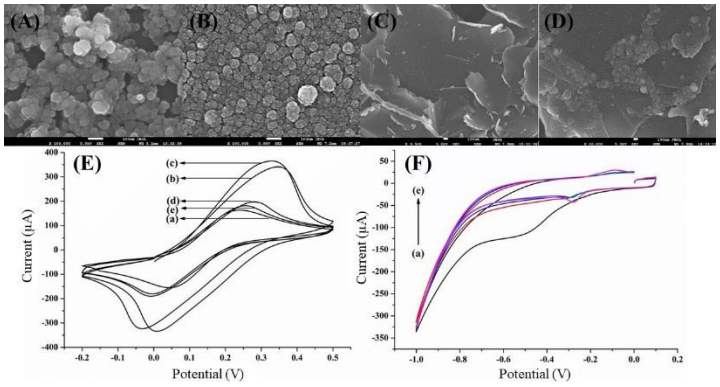

Figure 1. *Characterization of nanomaterials and food biosensor fabrication*: (A) SEM image of Fe_3O_4 nanoparticles; (B) SEM image of Fe_3O_4-Pd nanomaterials; (C) SEM image of bare SPGE; (D) SEM image of Fe_3O_4-Pd/CS nanocomposite modified SPGE; (E) CV of layer-by-layer fabrication study of the food biosensor fabrication, (a) bare SPGE, (b) SPGE/Fe_3O_4-Pd/CS, (c) SPGE/Fe_3O_4-Pd/CS/ABA, (d) SPGE/Fe_3O_4-Pd/CS/ABA/Ova-Ab, and (e) SPGE/Fe_3O_4-Pd/CS/ABA/Ova-Ab/BSA; and (F) CV cycles for electrografting of 4-ABA in 1 M HCl between -1 to 0.1 V at 200 mV/s, (a) 1st cycle – (e) 5th cycle

3.2. Layer-by-layer fabrication study of the food biosensor.

Cyclic voltammetry (CV) is a common technique to determine the electrochemical behavior of the electrode. Therefore, in this study, CV was used to monitor the layer-by-layer successful fabrication of the biosensor by determining the electro-active characteristics of the: (a) bare SPGE, (b) SPGE/Fe_3O_4-Pd/CS, (c) SPGE/Fe_3O_4-Pd/CS/ABA, (d) SPGE/Fe_3O_4-Pd/CS/ABA/mAb, (e) SPGE/Fe_3O_4-Pd/CS/ABA/Ova-Ab/BSA. When the Fe_3O_4-Pd/CS were drop-casted onto the working electrode surface of bare SPGE [Figure 1E, curve (b)], the peak currents were increased compared to the bare graphene [Figure 1E, curve (a)]. This demonstrated that Fe_3O_4-Pd/CS enhanced the electron transfer on the modified electrode suggesting that the metallic nanocomposite enhanced the redox processes. Furthermore, chitosan acts as the electron-bridge between the electrode surface, the bimetallic Fe_3O_4-Pd nanomaterials and the redox buffer, thus further enhanced the electron movement [31]. After one cycle of electrografting 4-ABA onto the modified electrode, the peaks were observed to increase further indicating that the grafted carboxyl phenyl film further enhances the electron transfer [Figure 1E, curve (c)]. In [Figure 1E, curve (d) and (e)] the peak currents decreased gradually when Ova-Ab, and BSA were added onto the surface of the electrode, suggesting the successful formation of the respective layers. The decrease in current indicated that the respective layers hindered the interfacial electron movement between the electrode surface and the redox buffer $[Fe(CN)_6]^{4-/3-}$. In this study, one cycle of carboxyphenyl film generated *in situ* from 4-ABA on the modified electrode was chosen between -1 to 0.1 V at scan rate of 200 mV/s as it is sufficiently being electrodeposited onto the electrode surface. A single irreversible cathodic peak at -0.5 V *vs* Ag/AgCl reference electrode was observed in the first cycle of the cyclic voltammetry (Figure 1F). The observed irreversible cathodic peak is derived from the reduction of carboxyphenyl diazonium salt that forms an aryl radical which covalently bonds onto the modified electrode surface [32]. Subsequent cycles of the electrodeposition resulted in saturation which is observed by a gradual decrease of the cathodic peak due to a thicker layer of diazonium film formed on the surface. Hence, one CV cycle was sufficient to effectively form a layer of carboxyl functionalization whilst ensuring an enhanced electrochemical profile for better sensitivity.

3.3. Optimisation of the food biosensor.

To maximise the analytical ability and stability of the food biosensor, several experimental parameters were optimized using DPV. These included the concentration of Ova-Ab, incubation time of Ova-Ab, blocking time, and antigen (Ova) – antibody (Ova-Ab) reaction time. The fabricated food biosensor was compared between without (0 pg/mL) and with (100 pg/mL) Ova using DPV for electronic current. A large change in current was calculated and chosen to maximize the maximum analytical sensing of the fabricated biosensor. A range of Ova-Ab concentrations was tested to determine the effect of different antibody concentrations on the biosensor. Figure 2A shows that, with increasing antibody concentrations (Ova-Ab), the current decreases. However, among the three fabricated food biosensors with three different Ova-Ab concentrations (1, 5 and 10 µg/mL) at same other experimental condition, the current change was maximum for the food biosensor fabricated with 5 µg/mL of Ova-Ab concentration, when tested without Ova (0 pg/mL) and with Ova (100 pg/mL) as shown in Figure 2A. This might be because, at higher Ova-Ab concentration (10 µg/mL), large number of Ova-Ab might have been accrued at the electrode surface resulting in lesser sensing current. Additionally accretion of the Ova-Ab concentration at the electrode surface could further decrease the active site for binding the Ova [33]. However, at 1 µg/mL of Ova-Ab, the current change was not observed as large because it is expected that with lower Ova-Ab concentration, lesser Ova will be detected. Therefore, as the food biosensor was designed to maximize the sensing ability, Ova-Ab concentration (5 µg/mL) was chosen as standard concentration to fabricate the food biosensor due to large current change between the fabricated biosensor without (0 pg/mL) and with (100 pg/mL) Ova. Further, food biosensor was also examined for the antibody incubation time. Three different incubation time (2, 6 and 14 h) was selected to study the maximum current change between the fabricated biosensors without (0 pg/mL) and with (100 pg/mL) Ova. While all the other experimental condition was maintained same. Ova-Ab incubated for 2 h for the fabrication of the biosensor demonstrated highest current change when tested without (0 pg/mL) and with (100 pg/mL) Ova as shown in Figure 2B. Therefore, 2 h was selected as standard time for the fabrication of the food biosensor for the detection of Ova.

Blocking is essential during fabrication of the biosensor to reduce non-specific binding of protein onto the electrode surface during analysis. Therefore, the blocking time by BSA was studied at 30, 45, and 60 mins maintaining the same experimental condition. The maximum current was observed for the 45 min as shown in Figure 2C. This indicate that the electrode surface was adequately blocked by BSA at 45 min. Therefore, 45 min was chosen a standard blocking time by BSA for the fabrication of the food biosensor. Finally, the four different reaction time (15, 30, 45 and 60) between Ova-Ab and Ova to form an immunocomplex was also examined. Among the four different tested time, biosensor demonstrated that immunocomplex formation reached to saturation point at 30 min and get stabilized (Figure 2D). The current at 15 min is highest, it could be due to not having sufficient immunocomplex formation time between the Ova and Ova-Ab at the biosensor. However saturation current for the formation of the immunocomplex at 45 and 60 min was indiscernible and lesser than the current at 30 min. It could be due to degradation of the Ova due to longer storage [33]. Therefore, 30 min was chosen as the optimal reaction time for the immunocomplex formation between the Ova and Ova-Ab.

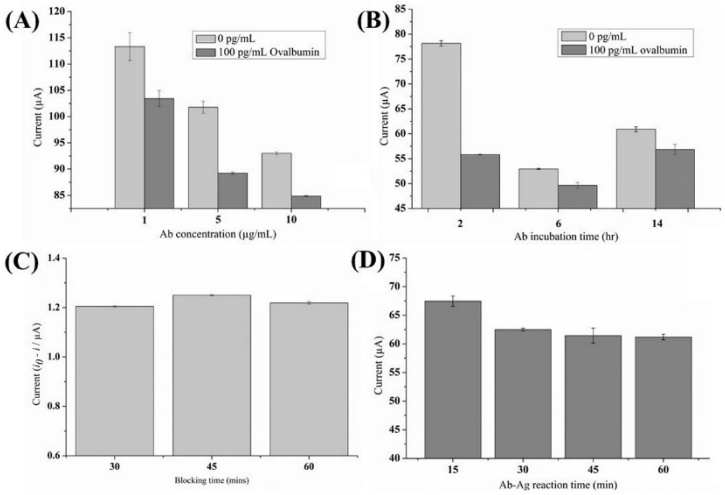

Figure 2. Optimization of experimental conditions: (A) The voltammetric current response of different antibody concentrations; (B) the current of the durations of antibody incubation time; (C) the reaction time of anti-OVA and OVA; (D) the blocking time with 0.1% BSA of the surface of the biosensor. (Error bars indicate the standard deviation from three experiments).

3.4. Analytical performance.

To investigate the analytical performance of the optimized fabricated food biosensor (SPGE/Fe_3O_4-Pd/CS/ABA/Ova-Ab/BSA), different concentrations (0 pg/mL to 1 µg/mL) of Ova food allergen were tested for detection under the optimized parameters (Ova-Ab concentration 5 µg/mL, Ova-Ab incubation time 2 h, blocking time by BSA 45 min, and immunocomplex formation time 30 min between Ova and Ova-Ab). DPV was used to monitor the immunocomplex formed between the Ova and Ova-Ab introduced onto the electrode surface. The determination of different concentrations of detected Ova was observed by the change in peak current of the redox probe $[Fe(CN)_6]^{4-/3-}$ on the electrode surface. A larger change in peak current was observed with increasing Ova concentration. This is because the formation of more immunocomplex impedes the movement of electron between the $[Fe(CN)_6]^{4-/3-}$ in the electrolyte and the surface of the electrode. Furthermore, Ova has an isoelectric point of 4.6 at pH 7.4 implying that the protein is negatively charged thus able to repel the anions of the redox buffer. Thus, as the concentration of Ova increases, more Ova would bind and impeded the electron movement between the $[Fe(CN)_6]^{4-/3-}$ in the electrolyte and electrode surface [6, 34]. As shown in Figure 3A, the DPV peak current decreased as the Ova concentrations were increased. A calibration curve was plotted to show the relationship between the change in peak current of the redox probe $[Fe(CN)_6]^{4-/3-}$ at varying concentrations of Ova and the logarithmic concentrations of Ova. A linear plot was procured with a large linearity range between 0.01 pg/mL to 1 µg/mL of Ova (Figure 3B). The limit of detection was 0.01 pg/mL, which was determined experimentally. The linear regression equation was $y = 2.3817x + 19.755$, $R^2 = 0.975$.

A comparison study for the performance of the biosensor and commercially available traditional ELISA kit (Veratox Egg Allergen) was carried out as shown in supplementary materials, Figure S-2. The ELISA kit has a detection limit of 100 ng/mL and

range of quantitation between 100 – 1000 ng/mL of egg protein. The nanocomposite (Fe_3O_4-Pd/CS) was proven to enhance the sensitivity and linearity of the food biosensor. The increase in sensitivity may be attributed to the nano-sized nanoparticles, which increased the surface area for the reaction to occur, and the combination of the synergistic effect of the bimetallic nanomaterials Fe_3O_4-Pd and the conducting polymers of CS and ABA [35].

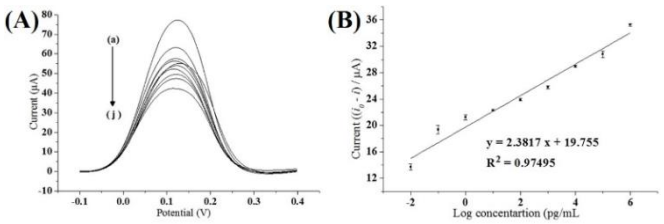

Figure 3. Calibration curves and Calibration plot: (A) DPV of the different concentrations of Ova. (a) 0 pg/mL, (b) 0.01 pg/mL, (c) 0.1 pg/mL, (d) 1 pg/mL, (e) 10 pg/mL, (f) 100 pg/mL, (g) 1 ng/mL, (h) 10 ng/mL, (i) 100 ng/mL, (j) 1µg/Ml; and (B) Calibration plot of the biosensor. (Error bars indicate the standard deviation from four experiments).

3.5. Reproducibility, stability, and selectivity.

The electrode-to-electrode reproducibility was investigated using four different modified electrodes (SPGE/Fe_3O_4-Pd/CS/ABA/Ova-Ab/BSA) for the detection of 100 pg/mL Ova (Figure 4A). The relative standard deviation (RSD) was 0.28% indicating a highly reproducible food biosensor. The long-term stability of the designed biosensor was also examined, whereby the electrodes were stored at 3 °C for a period of 20 days and the current measured at 4 days intervals. As depicted in Figure 4B, the current remained constant by the 4th day, but gradually decreased after the 12th day with only a slight drop in current by 1.1%. The food biosensor was still stable by the 20th day retaining 96.3% of the initial current signal. The stability of the biosensor may be attributed to the utilization of CS and ABA [36, 37]. To investigate the selectivity of the designed food biosensor, different food allergen proteins was tested (BSA, lysozyme, and casein). As illustrated in Figure 4C, the % decrease of the current signal for the other food proteins were significantly lower compared to OVA, suggesting an excellent selectivity for the fabricated food biosensor.

3.6. Spike and recovery analysis.

Analysis in food sample was carried out to test the application of the food biosensor to detect Ova with the effect of food matrix sample. The recoveries of three different spiked concentrations of Ova in the food sample was detected using three food biosensors. As shown in Table 1, the % recovery of concentrations were between 101.6% - 107.0% with RSD ranged from 5.0% to 6.2%. These data indicate that the designed food biosensor has non-significant effect of the matrix and portray feasibility for application in the detection of Ova in food sample.

Table 1. Spike-and-recovery assay using of the food biosensor

Spiked concentration (pg/mL)	Detected concentration (pg/mL)	Recovery (%)	RSD (%)
0.1	0.1030	103.0	5.0
10	10.70	107.0	6.2
10000	10160	101.6	5.7

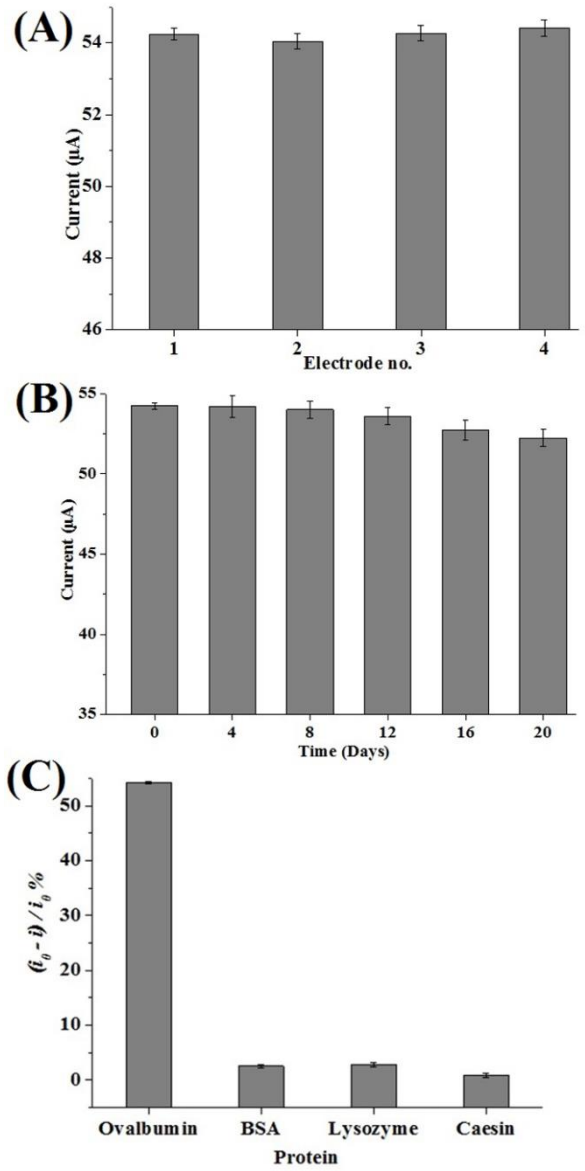

Figure 4. Reproducibility, stability and selectivity: (A) Reproducibility of the fabricated food biosensor to different electrodes detecting 100 pg/mL Ova; (B) The stability study of the fabricated food biosensor; (C) The selectivity of the food biosensor against three other common food allergen measured in % current decrease (i_0, blank; i, measured current). (Error bars indicate the standard deviation from three experiments).

4. CONCLUSIONS

A highly sensitive food biosensor utilizing Fe_3O_4-Pd/CS/ABA nanocomposite was fabricated onto graphene SPE for the voltammetric detection of ovalbumin with very large linearity between 0.01 pg/mL to 1 µg/mL and very low detection limit of 0.01 pg/mL. The designed Fe_3O_4/Pd/CS/ABA nanocomposite effectively enhanced the electroconductivity of the biosensor with excellent long-term stability and selectivity. Furthermore, the designed food biosensor has the potential for the application of ovalbumin in food samples.

5. REFERENCES

1. Tang, M.L.K.; Mullins, R.J. Food allergy: is prevalence increasing? *Intern. Med. J.* **2017**, *47*, 256-261, https://doi.org/10.1111/imj.13362.
2. Kato, Y.; Oozawa, E.; Matsuda, T. Decrease in Antigenic and Allergenic Potentials of Ovomucoid by Heating in the Presence of Wheat Flour: Dependence on Wheat Variety and Intermolecular Disulfide Bridges. *J. Agric. Food Chem.* **2001**, *49*, 3661-3665, https://doi.org/10.1021/jf0102766.
3. Maehashi, K.; Matano, M.; Irisawa, T.; Uchino, M.; Itagaki, Y.; Takano, K.; Kashiwagi, Y.; Watanabe, T. Primary Structure of Potential Allergenic Proteins in Emu (Dromaius novaehollandiae) Egg White. *J. Agric. Food Chem.* **2010**, *58*, 12530-12536, https://doi.org/10.1021/jf103239v.
4. Rizwan, M.; Koh, D.; Adela, B.M.; Ahmed, M.U. Combining a gold nanoparticle-polyethylene glycol nanocomposite and carbon nanofiber electrodes to develop a highly sensitive salivary secretory Immunoglobulin A immunosensor. *Sensors and Actuators B: Chemical* **2018**, *255*, 557-563, https://doi.org/10.1016/j.snb.2017.08.079.
5. Rizwan, M.; Elma, S.; Lim, S.A.; Ahmed M.U. AuNPs/CNOs/SWCNTs/chitosan-nanocomposite modified electrochemical sensor for the label-free detection of carcinoembryonic antigen. *Biosens. Bioelectron.* **2018**, *107*, 211-217, https://doi.org/10.1016/j.bios.2018.02.037.
6. Lim, S.A.; Ahmed, M.U. A carbon nanofiber-based label free immunosensor for high sensitive detection of recombinant bovine somatotropin. *Biosens. Bioelectron.* **2015**, *70*, 48-53, https://doi.org/10.1016/j.bios.2015.03.022.
7. Sun, Z.; Ge, H.; Hu, X.; Peng, Y. Preparation of foam-nickel composite electrode and its application to 2,4-dichlorophenol dechlorination in aqueous solution. *Sep. Purif. Technol.* **2010**, *72*, 133-139, https://doi.org/10.1016/j.seppur.2010.01.014.
8. Pikna, L.; Heželová, M.; Milkovič, O.; Smrčová, M. Study on electrochemical properties of Pd-C and Pd-CNT catalysts. *Part. Sci. Technol.* **2018**, *3*, 1-9., https://doi.org/10.1080/02726351.2018.1445151.
9. Ji, Y.; Liu, J.; Liu, X.; Yuen, M.M.F.; Fu, X.Z.; Yang, Y.; Sun, R.; Wong, C.P. 3D porous Cu@Cu2O films supported Pd nanoparticles for glucose electrocatalytic oxidation. *Electrochim Acta* **2017**, 248, 299-306, https://doi.org/10.1016/j.electacta.2017.07.100.
10. Uberman, P.M.; Pérez, L.A.; Martín, S.E.; Lacconi, G.I. Electrochemical synthesis of palladium nanoparticles in PVP solutions and their catalytic activity in Suzuki and Heck reactions in aqueous medium. *RSC Adv*. **2014**, *4*, 12330-12341, https://doi.org/10.1039/C3RA47854H.
11. Rajkumar, C.; Veerakumar, P.; Chen, S.M.; Thirumalraj, B.; Liu, S.B. Facile and novel synthesis of palladium nanoparticles supported on a carbon aerogel for ultrasensitive electrochemical sensing of biomolecules. *Nanoscale* **2017**, *9*, 6486-96, https://doi.org/10.1039/C7NR00967D.
12. Yang, C.C.; Kumar, A.S.; Zen, J.M. Electrocatalytic Reduction and Determination of Dissolved Oxygen at a Preanodized Screen-Printed Carbon Electrode Modified with Palladium Nanoparticles. *Electroanalysis* **2006**, *18*, 64-9, https://doi.org/10.1002/elan.200503374.
13. Hu, X.; Saran, A.; Hou, S.; Wen, T.; Ji, Y.; Liu, W.; Zhang, H.; He. W.; Yin. J.J.; Wu, X. Au@ PtAg core/shell nanorods: tailoring enzyme-like activities via alloying. *RSC. Adv.* **2013**, *3*, 6095-6105, https://doi.org/10.1039/C3RA23215H.
14. Li, A.; Zhao, X.; Hou, Y.; Liu, H.; Wu, L.; Qu, J. The electrocatalytic dechlorination of chloroacetic acids at electrodeposited Pd/Fe-modified carbon paper electrode. *Appl. Catal. B. Environ.* **2012**, *111-112*, 628-35, https://doi.org/10.1016/j.apcatb.2011.11.016.
15. Mohamad, N.N.; Abdul, R.K.; Lockman, Z. Physical and Electrochemical Properties of Iron Oxide Nanoparticles-modified Electrode for Amperometric Glucose Detection. *Electrochim Acta* **2017**, *248*, 160-168, https://doi.org/10.1016/j.electacta.2017.07.097.
16. Noorbakhsh, A.; Khakpoor, M.; Rafieniya, M.; Sharifi, E.; Mehrasa, M. Highly Sensitive Electrochemical Hydrogen Peroxide Sensor Based on Iron Oxide-Reduced Graphene Oxide-Chitosan Modified with DNA-Celestine Blue. *Electroanalysis* **2017**, *29*, 1113-1123, https://doi.org/10.1002/elan.201600660.
17. Sheng, W.; Xu, Q.; Chen, J.; Wang, H.; Ying, Z.; Gao, R.; Zheng, X.; Zhao, X. Electrochemical sensing of hydrogen peroxide using nitrogen-doped graphene/porous iron oxide nanorod composite. *Mater. Lett.* **2019**, *235*, 137-140, https://doi.org/10.1016/j.matlet.2018.10.022.
18. Tian, L.; Qi, J.; Oderinde, O.; Yao, C.; Song, W.; Wang, Y. Planar intercalated copper (II) complex molecule as small molecule enzyme mimic combined with Fe_3O_4 nanozyme for bienzyme synergistic catalysis applied to the microRNA biosensor. *Biosens. Bioelectron.* **2018**, *110*, 110-117, https://doi.org/10.1016/j.bios.2018.03.045.
19. Zhuang, L.; Tang, J.; Wang, Y.; Hu, M.; Zhou, S. Conductive iron oxide minerals accelerate syntrophic cooperation in methanogenic benzoate degradation. *J. Hazard. Mater.* **2015** *293*, 37-45, https://doi.org/10.1016/j.jhazmat.2015.03.039.
20. Yan, Q.; Yang, Y.; Tan, Z.; Liu, Q.; Liu, H.; Wang, P.; Chen, L.; Zhang, D.; Li, Y.; Dong, Y. A label-free electrochemical immunosensor based on the novel signal amplification system of AuPdCu ternary nanoparticles functionalized polymer nanospheres. *Biosens. Bioelectron*. **2018**, *103*, 151-157, https://doi.org/10.1016/j.bios.2017.12.040.
21. Shi, Q.; Wang, H.; Liu, S.; Pang, L.; Bian, Z. Electrocatalytic Reduction-oxidation of Chlorinated Phenols using a Nanostructured Pd-Fe Modified Graphene Catalyst. *Electrochim Acta* **2015**, *178*, 92-100, https://doi.org/10.1016/j.electacta.2015.07.186.
22. Song, X.; Shi, Q.; Wang, H.; Liu, S.; Tai, C.; Bian, Z. Preparation of Pd-Fe/graphene catalysts by photocatalytic reduction with enhanced electrochemical oxidation-reduction properties for chlorophenols. *Appl. Catal. B. Environ.* **2017,** *203*, 442-451, https://doi.org/10.1016/j.apcatb.2016.10.036.
23. Rajabzade, H.; Daneshgar, P.; Tazikeh, E.; Mehrabian, R.Z. Functionalized Carbon Nanotubes with Gold Nanoparticles to Fabricate a Sensor for Hydrogen Peroxide Determination. *E-Journal Chem.* **2012**, *9*, 2540-2549, http://dx.doi.org/10.1155/2012/157606.
24. Sarkar, S.; Guibal, E.; Quignard, F.; Sen Gupta, A.K. Polymer-supported metals and metal oxide nanoparticles: Synthesis, characterization, and applications. *J. Nanoparticle Res.* **2012**, *14*, 1-24, https://doi.org/10.1007/s11051-011-0715-2.
25. Suginta, W.; Khunkaewla, P.; Schulte, A. Electrochemical Biosensor Applications of Polysaccharides Chitin and Chitosan. *Chem. Rev.* **2013**, *113*, 5458-5479, https://doi.org/10.1021/cr300325r.
26. Fang, Y.; Zhang, D.; Guo, Y.; Guo, Y.; Chen, Q. Simple one-pot preparation of chitosan-reduced graphene oxide-Au nanoparticles hybrids for glucose sensing. *Sensors Actuators B Chem.* **2015**, *221*, 265-272, https://doi.org/10.1016/j.snb.2015.06.098.
27. Aziz, S.B. Morphological and Optical Characteristics of Chitosan((1-x)):Cu(o)(x) ($4 \leq x \leq 12$) Based Polymer Nano-Composites: Optical Dielectric Loss as an Alternative Method for Tauc's Model. Nanomaterials **2017**, *7*, 1-15, https://doi.org/10.3390/nano7120444.

28. Khiar, A.S.A.; Puteh, R.; Arof, A.K. Conductivity studies of a chitosan-based polymer electrolyte. *Phys. B. Condens. Matter.* **2006**, *373*, 23-27, https://doi.org/10.1016/j.physb.2005.10.104.
29. Lim, S.A.; Yoshikawa, H.; Tamiya, E.; Yasin, H.M.; Ahmed, M.U. A highly sensitive gold nanoparticle bioprobe based electrochemical immunosensor using screen printed graphene biochip. *RSC. Adv.* **2014**, *4*, 58460-58466, https://doi.org/10.1039/C4RA11066H.
30. Jing, H.; Wang, H. Controlled overgrowth of Pd on Au nanorods. *Cryst. Eng. Comm.* **2014**, *16*, 9469-9477, https://doi.org/10.1039/C4CE00601A.
31. Cheng, H.Y.; Hou, Y.N.; Zhang, X.; Yang, Z.N.; Xu, T.; Wang, A.J. Activating electrochemical catalytic activity of bio-palladium by hybridizing with carbon nanotube as "e− Bridge." *Sci. Rep*. **2017**, *7*, 1-9, https://doi.org/10.1038/s41598-017-16880-7.
32. Eissa, S.; L'Hocine, L.; Siaj, M.; Zourob, M. A graphene-based label-free voltammetric immunosensor for sensitive detection of the egg allergen ovalbumin. *Analyst* **2013**, *138*, 4378-4384, https://doi.org/10.1039/C3AN36883A.
33. Islam, F.; Haque, M.H.; Yadav, S.; Islam, M.N.; Gopalan, V.; Nguyen, N.T.; Lam, A.K.; Shiddiky, M.J.A. An electrochemical method for sensitive and rapid detection of FAM134B protein in colon cancer samples. *Sci. Rep.* **2017**, *7*, 1-9, https://doi.org/10.1038/s41598-017-00206-8.
34. Yadav, S.; Carrascosa, L.G.; Sina, A.A.I.; Shiddiky, M.J.A.; Hill, M.M.; Trau, M. Electrochemical detection of protein glycosylation using lectin and protein-gold affinity interactions. *Analyst* **2016**, *141*, 2356-2361, https://doi.org/10.1039/C6AN00528D.
35. Liu, D.; Xie, ML.; Wang, CM.; Liao, L.W.; Qiu, L.; Ma. J.; Huang, H.; Long, R.; Jiang, J.; Xiong, Y. Pd-Ag alloy hollow nanostructures with interatomic charge polarization for enhanced electrocatalytic formic acid oxidation. *Nano Res.* **2016**, *9*, 1590-1599, https://doi.org/10.1007/s12274-016-1053-6.
36. Giannetto, M.; Costantini, M.; Mattarozzi, M.; Careri, M. Innovative gold-free carbon nanotube/chitosan-based competitive immunosensor for determination of HIV-related p24 capsid protein in serum. *RSC Adv.* **2017**, *7*, 39970-39976, https://doi.org/10.1039/C7RA07245G.
37. Suresh, L.; Brahman, P.K.; Reddy, K.R.; Bondili, J.S. Development of an electrochemical immunosensor based on gold nanoparticles incorporated chitosan biopolymer nanocomposite film for the detection of prostate cancer using PSA as biomarker. *Enzyme Microb. Technol.* **2018**, *112*, 43-51. https://doi.org/10.1016/j.enzmictec.2017.10.009.

6. ACKNOWLEDGEMENTS

Azureen Mohamad wishes to thank the Ministry of Education of Brunei Darussalam for her Ph.D. fellowship. This work was partly supported by the Universiti Brunei Darussalam's grant UBD/RSCH/1.4/FICBF(b)/2018/010.

Supplementary Materials

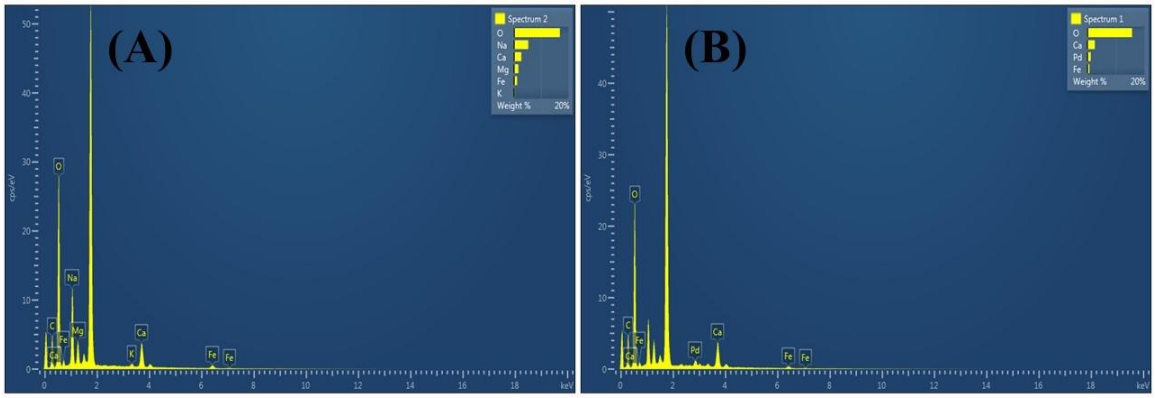

Figure S1. EDX spectra of nanomaterials: (A) Fe_3O_4 nanoparticles; (B) Fe_3O_4/Pd nanocomposite.

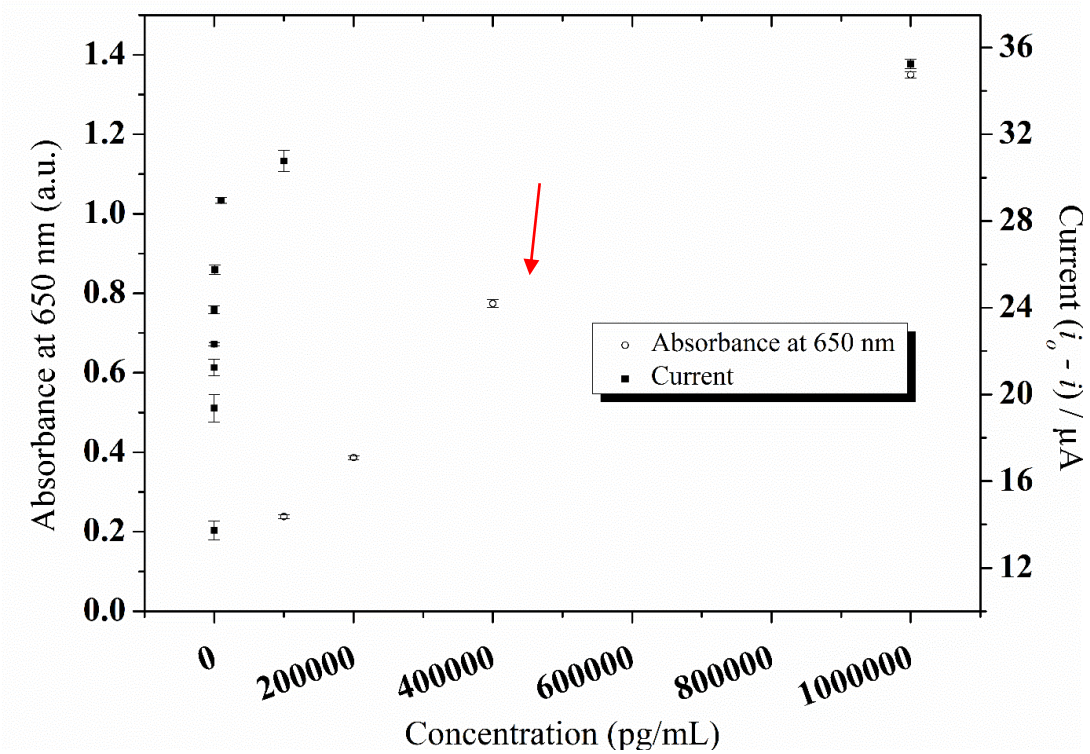

Figure S-2. Comparison of ELISA kit with the designed food biosensor.